



## Soil moisture retrieval algorithm using Sentinel-1 images

Nicolas Baghdadi, Mohammad El Hajj, Mehrez Zribi

### ► To cite this version:

Nicolas Baghdadi, Mohammad El Hajj, Mehrez Zribi. Soil moisture retrieval algorithm using Sentinel-1 images. International Scientific and Practical Conference “Problems of Desertification: Dynamics, Assessment, Solutions”, Dec 2019, Samarkand, Uzbekistan. hal-02631815

HAL Id: hal-02631815

<https://hal.inrae.fr/hal-02631815v1>

Submitted on 27 May 2020

**HAL** is a multi-disciplinary open access archive for the deposit and dissemination of scientific research documents, whether they are published or not. The documents may come from teaching and research institutions in France or abroad, or from public or private research centers.

L'archive ouverte pluridisciplinaire **HAL**, est destinée au dépôt et à la diffusion de documents scientifiques de niveau recherche, publiés ou non, émanant des établissements d'enseignement et de recherche français ou étrangers, des laboratoires publics ou privés.

# Soil moisture retrieval algorithm using Sentinel-1 images

Nicolas Baghdadi<sup>1</sup>, Mohammad El Hajj<sup>1</sup>, Mehrez Zribi<sup>2</sup>

<sup>1</sup> TETIS, IRSTEA, University of Montpellier, 34090 Montpellier, France

<sup>2</sup> CESBIO (CNRS/UPS/IRD/CNES), 31401 Toulouse CEDEX 9, France

## ABSTRACT

The aim of this communication is to present an operational approach for mapping soil moisture at high spatial resolution (plot scale) in agriculture areas by coupling S1 and S2 images. The proposed approach is based on the inversion of the Water Cloud Model (WCM) combined with the modified Integral Equation Model (IEM). Neural networks were developed and validated using synthetic SAR C-band database. The results showed that the soil moisture could be estimated in agricultural areas with an accuracy of approximately 5 vol.%.

**Index Terms** - Soil moisture, Sentinel-1&2, SAR, C-band, Neural networks.

## 1. INTRODUCTION

Soil moisture content and surface roughness play an important role in meteorology, hydrology, agronomy, agriculture, and risk assessment. These soil surface characteristics can be estimated using synthetic aperture radar (SAR) [1-17]. SAR data in the C- and X-bands were widely and primarily used to estimate surface soil moisture (SSM) over bare soils and soils covered with vegetation. The arrival of free and open access Sentinel-1 "S1" (10 m spatial resolution and a 6-day revisit period) and Sentinel-2 "S2" (10 m spatial resolution and a 6-day revisit period) satellites have encouraged the development of operational algorithms for soil moisture mapping over agricultural areas with high revisit time (6 days with the two Sentinel-1 satellites) and high spatial resolution (up to plot scale).

The retrieval of soil moisture content and surface roughness requires the use of radar backscatter models capable of correctly modeling the radar signal for a wide range of soil parameter values. This estimation from imaging radar data implies the use of backscattering electromagnetic models, which can be physical, semi-empirical or empirical [18-20].

Several studies tend to use the neural networks technique to invert backscattering models and estimate the soil moisture. To estimate soil moisture and roughness over bare soils from the C-band polarimetric radar data, Baghdadi et al. [8] first generated a database of backscattering coefficients for a wide range of bare soil conditions ( $H_{rms}$  between 0.3 and 3.6 cm and SSM between 5 and 45 vol.%) using the Integral Equation Model IEM [18-19]. Then, the neural networks (NNs) were trained using the synthetic database. Finally, the trained neural networks were validated using a real database.

The aim of this paper is to present an operational approach for mapping soil moisture at high spatial resolution (up to the plot scale) in agriculture areas by coupling S1 and S2 images. The proposed approach uses the neural network technique [8,21]. It is based on the inversion of the WCM combined with the modified Integral Equation Model (IEM) [18-19].

## 2. S1-SSM ALGORITHM

The approach for soil moisture mapping uses the neural networks (NNs) technique to invert the radar backscattering signal [2]. It uses the Water Cloud Model parameterized by Baghdadi et al. [22] for the C-band combined with the Integral Equation model (IEM) [18,23]. The total radar backscattering coefficient in the WCM is considered as the sum of the direct vegetation contribution and the soil contribution multiplied by the attenuation factor. Using a vegetation descriptor (NDVI) derived from optical images (Sentinel-2), the direct contribution of vegetation as well as the attenuation of soil scattering can be computed.

The development of the inversion method consists of the following steps [2]:

- Generate a synthetic database of backscattering coefficients in VV polarization ( $\sigma^{\circ}\text{VV}$ ) using a parameterized WCM combined with the modified IEM;
- Noise the synthetic SAR C-band database (zero-mean Gaussian random additive noises with a standard deviation of  $\pm 0.7$  and  $\pm 1.0$  dB to be added to the simulated backscattering coefficients in VV, respectively) and NDVI values (zero-mean Gaussian additive relative noise of 15%) to obtain synthetic database close to the real SAR and NDVI data;
- Train and validate the neural networks using the noisy synthetic dataset;
- Finally, apply the trained neural networks to S1 and S2 images to map the soil moisture.

Wide range of incidence angle " $\theta$ " ( $20^{\circ}$  to  $45^{\circ}$ ), SSM (2 to 40 vol. %),  $Hrms$  (0.5 to 3.8 cm), and NDVI (0 to 0.75) was considered in the generation of synthetic SAR database. Each element of the database is composed of a combination of four input parameters  $\theta$ , SSM,  $Hrms$ , NDVI and a simulated  $\sigma^{\circ}\text{VV}$ . Two SAR configurations for estimating the soil moisture are considered:

- Configuration 1: incidence angle, noisy radar signal at VV polarization, and noisy NDVI are the inputs of the NNs;
- Configuration 2: incidence angle, both noisy radar signal at VV polarization and noisy NDVI are the inputs of the NNs.

The soil roughness (root mean square surface height “ $Hrms$ ”) was not used as an input parameter for the neural networks training and validation. NNs were trained in using the Levenberg-Marquardt algorithm with two hidden layers. The number of neurons for each hidden layer is 20. Linear and tangent-sigmoid transfer functions were associated with the first and second hidden layers, respectively.

### 3. RESULTS

Figures 1a and 1b show the performance of the neural networks that take  $\sigma^{\circ}\text{vv}$ ,  $\theta$ , and NDVI as input parameters (configuration 1). For a reference SSM lower than 25 vol.% (dry to wet soils), small bias "estimated SSM – reference SSM" (1.2 vol.%) and RMSE of 4.0 vol.% are observed (Figure 1a). Similarly, for a reference SSM between 25 and 40 vol.% (very wet conditions), a bias of -2.3 vol.% and an RMSE of 5.1 vol.% are obtained (Figure 1b).

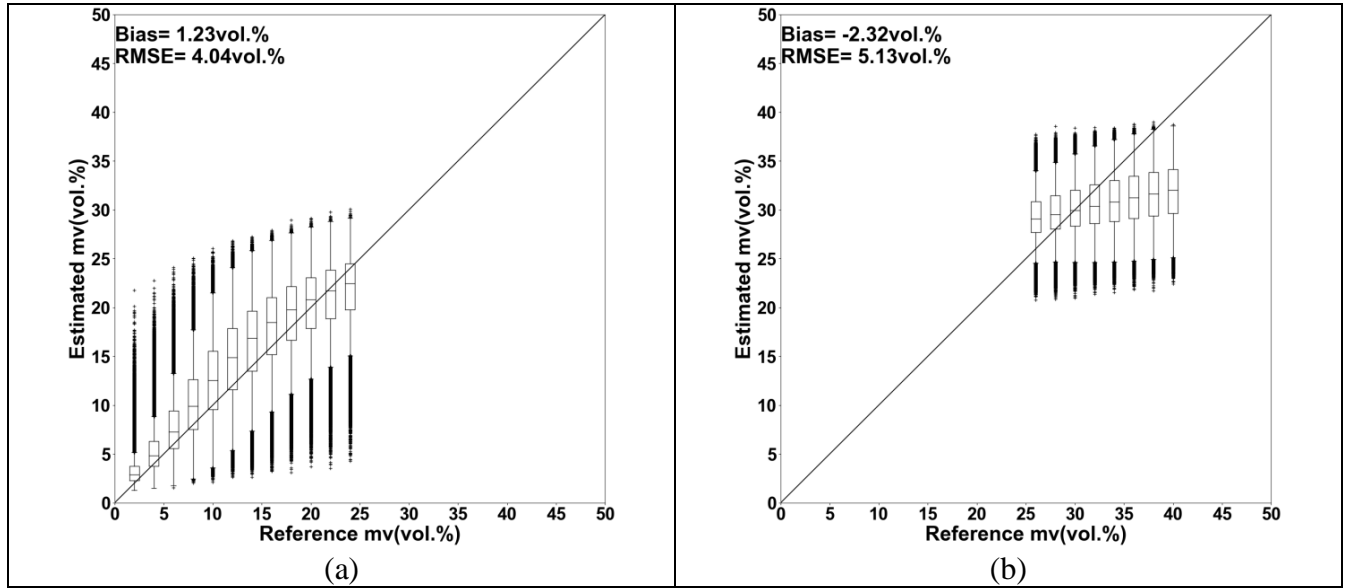


**Figure 1.** Estimated SSM as a function of the reference SSM. (a) VV is used alone, dry to wet soils, (b) VV is used alone, very wet soils.

The approach for the operational mapping of soil moisture was applied over a study site located in Occitanie, South France (Figure 2). S1-SSM maps are available at high spatial resolution (up to plot scale) since September 2016 as open access data via the Theia French Land Data Center (<http://www.theia-land.fr/en/thematic-products>). An evaluation of SMOS, SMAP, ASCAT and S1-SSM products was performed by El Hajj et al. [24] and reveals that the S1-derived soil moisture maps provide the most accurate estimation of SSM. The higher accuracy of estimated SSM moisture is probably due to the well-calibrated IEM combined with the well parameterized WCM and the use of high spatial resolution ( $10\text{ m} \times 10\text{ m}$ ) land cover maps derived from S2 images to eliminate SAR scattering from forest and urban areas.

A comparison between S1-SSM maps and precipitation derived from GPM (Global Precipitation Measurement) data was carried out. For each S1-SSM map date, one cumulative rainfall map for the 6 days prior to the S1-SSM map date was computed by summing the 30 min time interval of the Late IMERG GPM product. Then, each S1-derived SSM map was overlaid with the corresponding 6 days of cumulative GPM rainfall. Starting with the initial map on 21/12/2016 (Figure 2a), departments as Tarn, Hérault, Lozère, and Aveyron of the eastern and middle parts of the region encountered high soil moisture values (more than 20 vol.%) corresponding to 10-20 mm cumulative precipitation during the past 6 days, whereas Gers and Haute-Garonne of the western part shows low soil moisture values (20 vol.% at most) corresponding to the absence of precipitation in the area for the same prior period. A

map derived 6 days later on 27/12/2016 (Figure 2b) shows a decrease in soil moisture values in the Hérault and Gard due to the absence of precipitation between 21/12/2016 and 27/12/2016. Moreover, high soil moisture values are estimated for Tarn due to continuous raining episodes between 21/12/2017 and 27/12/2017, and a slight increase in soil moisture values is observed in western part due to 3 mm of precipitation recorded one day prior to the S1-SSM map according to the GPM data (Figure 2b). A general decrease in soil moisture values throughout the region is observed between 27/12/2016 (Figure 2b) and 02/01/2017 (Figure 2c) as no precipitation was recorded. A continuous lack of precipitation for 12 days from 27/12/2016 until 08/01/2017 caused soil moisture values to drop to less than 15 vol.% on 08/01/2017 in the whole region as shown in Figure 2d. Six days later on 14/01/2017 (Figure 2e), soil moisture values remained low at the east as no precipitation was recorded for an additional 6 days, whereas a moderate increase in soil moisture values is observed in the middle and western parts (Tarn, Haute-Garonne, and Gers) corresponding to precipitation between 08/01/2017 and 14/01/2017 (a cumulative rainfall increase of 5-20 mm). Twenty-four days with no precipitation recorded in the Hérault and Gard region between 27/12/2016 and 20/01/2017 caused the soil moisture values to drop more, with values less than 15 vol.% in this area on 20/01/2017 (Figure 2f).

In addition, for Gers department, low soil moisture values (less than 15 vol.%) were estimated on January 20, 2017 and high cumulative precipitation was recorded between 14 and 20 January 2017 (15 mm) (Figure 2f). This low soil moisture estimates could be linked to the presence of frozen soil in the area. In a recent study using Sentinel-1 SAR data, Baghdadi et al. [25] showed that a decrease of at least 3 dB in the radar backscattered signal can be observed over frozen soil conditions. Such a decrease in the SAR signal yields an underestimation of soil moisture in the S1-derived SSM maps. In our case, it seems that low soil moisture values for this area on 20/01/2017, although with the presence of rainfall, is due to frozen soil conditions. To support our assumption, the temperature curve and precipitation records for a local meteorological station in Auch city located in Gers-Occitanie were analyzed. On 19 January 2017 (S1 acquisition over Gers on January 19, 2017 17:56 UTC), the temperature varied between -8°C and 2°C with a mean value of -3°C throughout the day. Three days before (15 and 16 January) 15 mm cumulative precipitation was recorded. Thus, a precipitation event followed by a decrease in the air temperature to less than 0°C justifies the presence of frozen soil conditions as the cause of a decrease in the estimated soil moisture values in the S1-derived SSM maps.

After 29 days of dry conditions in the eastern part (Hérault and Gard between 27/12/2016 and 25/01/2017), a sudden increase in the soil moisture was observed on 26/01/2017 with the beginning of a rainfall event (Figure 2g). The mean S1-SSM mean value in this area increased from 13 vol.% in 20/01/2017 to 32 vol.% in 26/01/2017. On the other hand, the absence of precipitation in the remaining parts of the region between 20/01/2017 and 26/01/2017 caused soil moisture to attain lower values (16 vol.%) on 26/01/2017. The slight increase in soil moisture values in Gers between 20 and 26 January is probably due to the disappearance of the frozen conditions observed in the previous acquisition (20/01/2017). The temporal analysis of S1-derived SSM values over a period of time shows the direct effect of raining episodes or dry conditions on S1-SSM values.

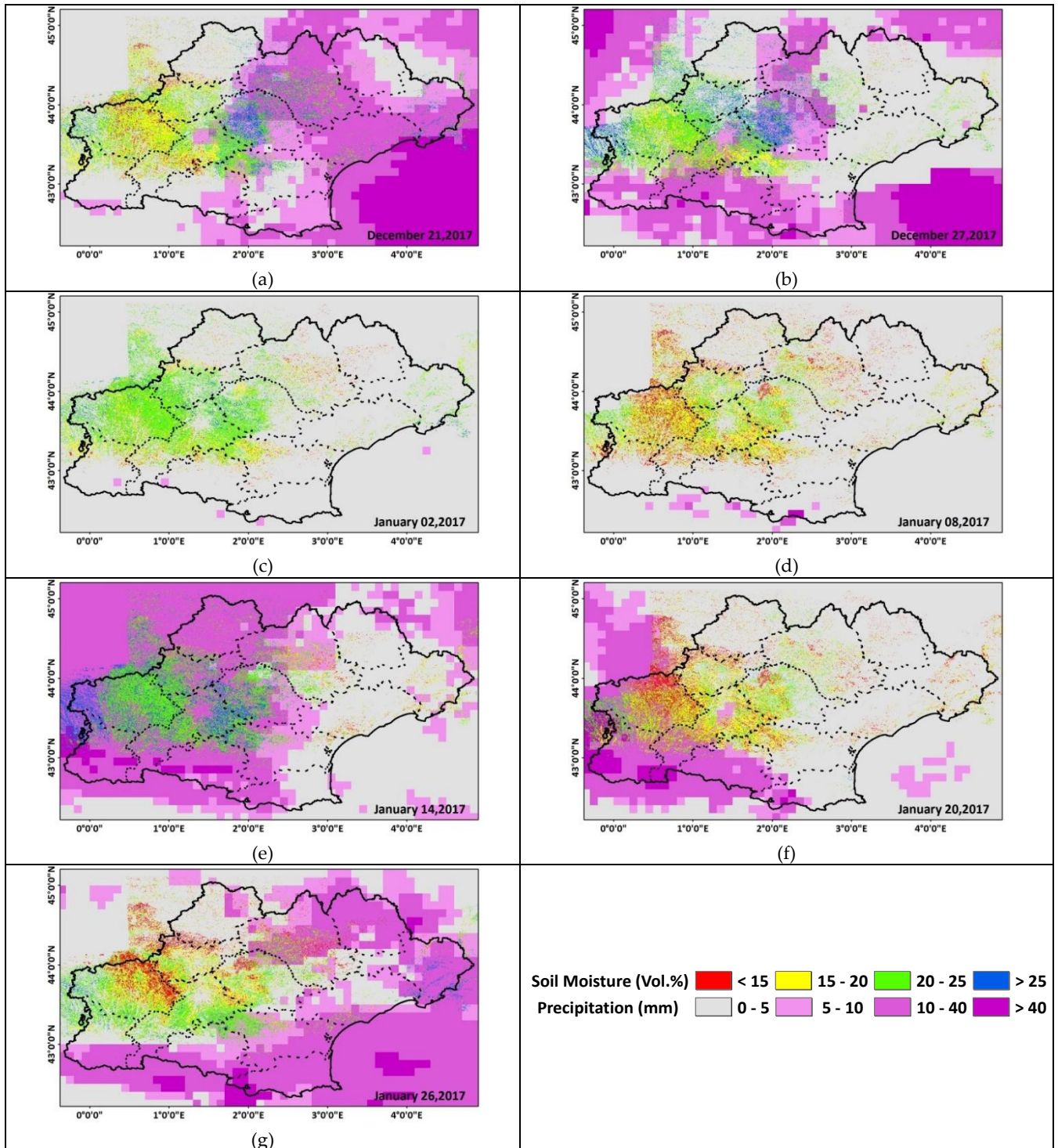


**Figure 2.** S1-derived SSM map overlaid with GPM cumulative precipitation data. (a) 21/12/2016, (b) 27/12/2016, (c) 02/01/2017, (d) 08/01/2017, (e) 14/01/2017, (f) 20/01/2017, (g) 26/01/2017.

## 4. CONCLUSION

This paper present an operational approach for soil moisture estimates in agricultural areas at a high spatial resolution (up to plot scale). Our approach is based on a synergic use of radar and optical images. With the use of Sentinel-1 and Sentinel-2 data, the developed approach will provide soil moisture mapping with a high temporal frequency. Our approach for soil moisture estimates used the neural networks technique to invert the radar signal and estimate the soil moisture.

From the synthetic database, the results showed that the soil moisture in agricultural areas could be estimated with an accuracy of approximately 5 vol.%. A good coherence was observed between the temporal evolution of the soil moisture and the precipitation records derived from the GPM data. The S1-SSM values increases following rainfall event and decreases after a period without rainfall due to evaporation.

## 5. ACKNOWLEDGMENT

This research was supported by IRSTEA (National Research Institute of Science and Technology for Environment and Agriculture) and the French Space Study Center (CNES, DAR 2019 TOSCA). The authors wish to thank the European Commission and the European Space Agency for providing the S1 images. We used Copernicus level 2A S2 data processed by Theia (<https://www.theia-land.fr>).

## 6. REFERENCES

1. Baghdadi N., El Hajj M., Choker M., Zribi M., Bazzi H., Vaudour E., Gilliot J.M., Dav M. Ebengo, 2018. Potential of Sentinel-1 images for estimating the soil roughness over bare agricultural soils. *Water*, 10, 131, pp. 1-14.
2. El Hajj M., Baghdadi N., Zribi M., Bazzi H., Synergic use of Sentinel-1 and Sentinel-2 images for operational soil moisture mapping at high spatial resolution over agricultural areas, *Remote Sensing*, 2017, 9, 1292.
3. Baghdadi N., El Hajj M., Zribi M., and Fayad I., 2016. Coupling SAR C-band and optical data for soil moisture and leaf area index retrieval over irrigated grasslands. *IEEE JSTARS*, vol. 9, no. 3, pp. 1229-1243.
4. El Hajj M., Baghdadi N., Zribi M., Belaud G., Cheviron B., Courault D., and Charron F., 2016. Soil moisture retrieval over irrigated grassland using X-band SAR data. *Remote Sensing of Environment*, vol. 176, pp. 202-218.
5. Aubert M., Baghdadi N., Zribi M., Ose K., El Hajj M., Vaudour E., and Gonzalez-Sosa E., 2013. Toward an operational bare soil moisture mapping using TerraSAR-X data acquired over agricultural areas, *IEEE Journal of Selected Topics in Applied Earth Observations and Remote Sensing (JSTARS)*, vol. 6, issue 2, pp. 900-916.
6. Baghdadi N., Dubois-Fernandez P., Dupuis X., and Zribi M., 2013. Sensitivity of polarimetric parameters of multifrequency polarimetric SAR data to soil moisture and surface roughness over bare agricultural soils. *IEEE Geoscience and Remote Sensing Letters*, vol. 10, no. 4, pp. 731-735.
7. Dong L., Baghdadi N., and Ludwig R., 2013. Retrieving surface soil moisture using radar imagery in a semi-arid environment. *IEEE Geoscience and Remote Sensing Letters*, vol. 10, no. 3, pp. 461-465.
8. Baghdadi N., Cresson R., El Hajj M., Ludwig R., and La Jeunesse I., 2012. Estimation of soil parameters over bare agriculture areas from C-band polarimetric SAR data using neural networks. *Hydrology and Earth System Sciences (HESS)*, vol. 16, pp. 1607-1621.
9. Baghdadi N., Aubert M., Zribi M., 2012. Use of TerraSAR-X data to retrieve soil moisture over bare soil agricultural fields. *IEEE Geoscience and Remote Sensing Letters*, vol. 9, no. 3, pp. 512-516.

10. Baghdadi N., Camus P., Beaugendre N., Malam Issa O., Zribi M., Desprats J.F., Rajot J.L., Abdallah C., and Sannier C, 2011. Estimating surface soil moisture from TerraSAR-X data over two small catchments in the sahelian part of western Niger. *Remote Sensing – Sensors*, vol. 3, pp. 1266-1283.
11. Aubert M., Baghdadi N., Zribi M., Douaoui A., Loumagne C., Baup F., El Hajj M., and Garrigues S., 2011. Analysis of TerraSAR-X data sensitivity to bare soil moisture, roughness, composition and soil crust, *Remote Sensing of Environment*, 115, pp. 1801-1810.
12. Baghdadi N., Zribi M., Loumagne C., Ansart P., and Paris Anguela T., 2008. Analysis of TerraSAR-X data and their sensitivity to soil surface parameters over bare agricultural fields. *Remote Sensing of Environment*, vol. 112, issue 12, pp. 4370-4379.
13. Baghdadi N., Cerdan O., Zribi M., Auzet V., Darboux F., El Hajj M., and Bou Keir R., 2008. Operational performance of current synthetic aperture radar sensors in mapping soil surface characteristics: application to hydrological and erosion modelling. *Hydrological Processes*, vol. 22, Issue 1, pp. 9-20.
14. Baghdadi N., Aubert M., Cerdan O., Franchistéguy L., Viel C., Martin E., Zribi M., and Desprats J.F., 2007. Operational mapping of soil moisture using synthetic aperture radar data: application to Touch basin (France). *Sensors Journal*, vol. 7, pp. 2458-2483.
15. Baghdadi N., Holah N., and Zribi M., 2006. Soil moisture estimation using multi-incidence and multi-polarization ASAR SAR data. *International Journal of Remote Sensing*, vol. 27, no. 10, pp. 1907–1920.
16. Holah H., Baghdadi N., Zribi M., Bruand A., and King C., 2005. Potential of ASAR/ENVISAT for the characterisation of soil surface parameters over bare agricultural fields. *Remote Sensing of Environment*, vol. 96, no. 1, pp. 78-86.
17. Baghdadi N., King C., Bourguignon A., and Remond A., 2002. Potential of ERS and RADARSAT data for surface roughness monitoring over bare agricultural fields : application to catchments in Northern France. *International Journal of Remote Sensing*, vol. 23, no. 17, pp. 3427-3442.
18. Baghdadi N., Holah N., and Zribi M., 2006. Calibration of the Integral Equation Model for SAR data in C-band and HH and VV polarizations. *International Journal of Remote Sensing*, vol. 27, no. 4, pp. 805-816.
19. Baghdadi N., King C., Chanzy A., and Wingneron J.P., 2002. An empirical calibration of IEM model based on SAR data and measurements of soil moisture and surface roughness over bare soils. *International Journal of Remote Sensing*, vol. 23, no. 20, pp. 4325-4340.
20. Baghdadi N., Choker M., Zribi M., El Hajj M., Paloscia S., Verhoest N., Lievens H., Baup F., Mattia F., 2016. A new empirical model for radar scattering from bare soil surfaces. *Remote Sensing*, vol. 8, Issue 11, pp. 1-14.
21. Baghdadi N., Gaultier S., and King C., 2002. Retrieving surface roughness and soil moisture from SAR data using neural network. *Canadian Journal of Remote Sensing*, vol. 28, no. 5, pp. 701-711.
22. Baghdadi, N.; El Hajj, M.; Zribi, M.; Bousbih, S. Calibration of the Water Cloud Model at C-Band for Winter Crop Fields and Grasslands. *Remote Sensing* 2017, 9, 969.
23. Baghdadi, N.; Abou Chaaya, J.; Zribi, M. Semi empirical Calibration of the Integral Equation Model for SAR Data in C-Band and Cross Polarization Using Radar Images and Field Measurements. *IEEE Geoscience and Remote Sensing Letters* 2011, 8, 14–18.
24. El Hajj, M.; Baghdadi, N.; Zribi, M.; Rodríguez-Fernández, N.; Wigneron, J.; Al-Yaari, A.; Al Bitar, A.; Albergel, C.; Calvet, J.-C. Evaluation of SMOS, SMAP, ASCAT and Sentinel-1 Soil Moisture Products at Sites in Southwestern France. *Remote Sensing* 2018, 10, 569.
25. Baghdadi, N.; Bazzi, H.; El Hajj, M.; Zribi, M. Detection of Frozen Soil Using Sentinel-1 SAR Data. *Remote Sensing* 2018, 10, 1182.